



# Heat Transfer Computational Project - Simulation of The Defrosting of a Car Rear Window

Raphael ALVES HAILER - [raphael.alves@ensta-paris.fr](mailto:raphael.alves@ensta-paris.fr)

Course: MF202

Professor: Patrice PARICAUD

Date: March 6, 2023

# Contents

<b>1</b>	<b>Numerical Description of The General Problem</b>	<b>3</b>
1.1	Finite Volumes Method . . . . .	3
<b>2</b>	<b>Numerical Simulation: Results</b>	<b>9</b>
<b>3</b>	<b>Experimenting With New Parameters</b>	<b>13</b>

## List of Figures

1	Illustration of the problem with generic mesh. . . . .	2
2	Spacial discretization of domain $\Omega$ . . . . .	3
3	Control volume for the interior nodes of $\Omega$ . . . . .	4
4	Control volume for the right boundary nodes of $\Omega$ . . . . .	5
5	Control volume for the upper boundary nodes of $\Omega$ . . . . .	7
6	Control volume for the top right corner node of $\Omega$ . . . . .	7
7	Temporal evolution of the temperature distribution on the car's rear window . . . . .	10
8	Temperature distribution at $t = 120$ s after correcting the aspect ratio of the x and y axis	11
9	Unstable response for inappropriate discretization values. . . . .	12
10	Comparison between rougher and finer mesh. . . . .	13
11	Temperature distribution after 120 seconds with $L_y = 2$ cm. . . . .	14
12	Temperature distribution after 120 seconds with $k = 2.52$ W/(m·K). . . . .	14

# Introduction

This computational project is focused on analysing the heat conduction inside a car rear window in a cold winter day, by using numerical methods to approximate our solution in the transient regime. The use of a numerical approach is necessary due to the complexity of the problem, and it gives us a good insight on how the window is behaving and to check if the provided heat is enough to defrost the car's window.

Consider the rear window of a car that consists of a 0.4 cm-thick glass ( $k = 0.84 \text{ W}/(\text{m}\cdot\text{K})$  and  $\alpha = 0.38 \times 10^{-6} \text{ m}^2/\text{s}$ ). Heating wires are attached to the inner surface of the glass, considered in our geometry to be the surface by the left, or the left boundary, while the surface by the right or the right boundary is exposed to exterior air. The wires are 4 cm apart from each other and they generate heat at a rate of  $25 \text{ W}/\text{m}$ , where the length considered to obtain the real heat generation in watts is the depth of the window.

Initially the entire car, including its windows, is at the outdoor temperature of  $T_0 = T_\infty = -3^\circ\text{C}$ . The heat transfer coefficients at the inner and outer surfaces of the glass can be taken to be  $h_i = 6 \text{ W}/(\text{m}^2\cdot\text{K})$  and  $h_o = 20 \text{ W}/(\text{m}^2\cdot\text{K})$ .

Since the heating wires are separated from each other in a symmetrical manner, we can take a vertical region of height 4cm where the wire is exactly at the center on the left boundary, because we can have thermal symmetry lines on the top and bottom boundaries, which facilitates the analysis. By using this symmetry, we can adopt adiabatic boundaries at the top and the bottom of our domain  $\Omega$ , meaning that there will be no heat flux vertically in these boundaries. An image of the described problem is shown, with a generic mesh, just to illustrate the problem's geometry

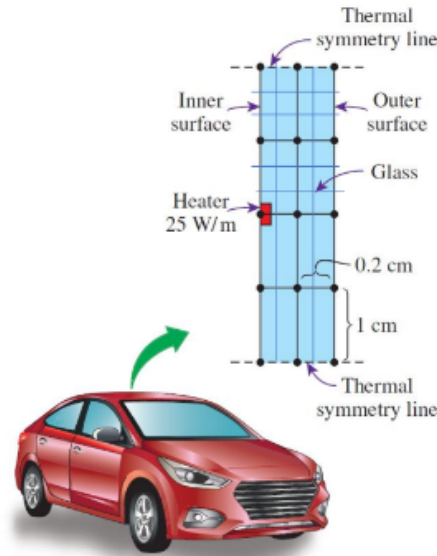


Figure 1: Illustration of the problem with generic mesh.

# 1 Numerical Description of The General Problem

In order to analyse the car rear window, we will be relying on the use of the finite volumes method. Firstly, a spacial and temporal discretization is necessary. Consider a rectangular domain  $\Omega$  of lengths  $L_x$  and  $L_y$  in the  $x$  and  $y$  directions, respectively. We will consider that we have  $n_x$  and  $n_y$  ordered points in the  $x$  and  $y$  directions, respectively, and that both sequences of points start at 1. Therefore,  $(x_1, y_1) = (0, 0)$  and  $(x_{n_x}, y_{n_y}) = (L_x, L_y)$ , in order to obtain a mesh in the Cartesian coordinate system.

Furthermore, we will consider that a generic point will have indices  $i$  and  $j$  in the horizontal and vertical directions, respectively.

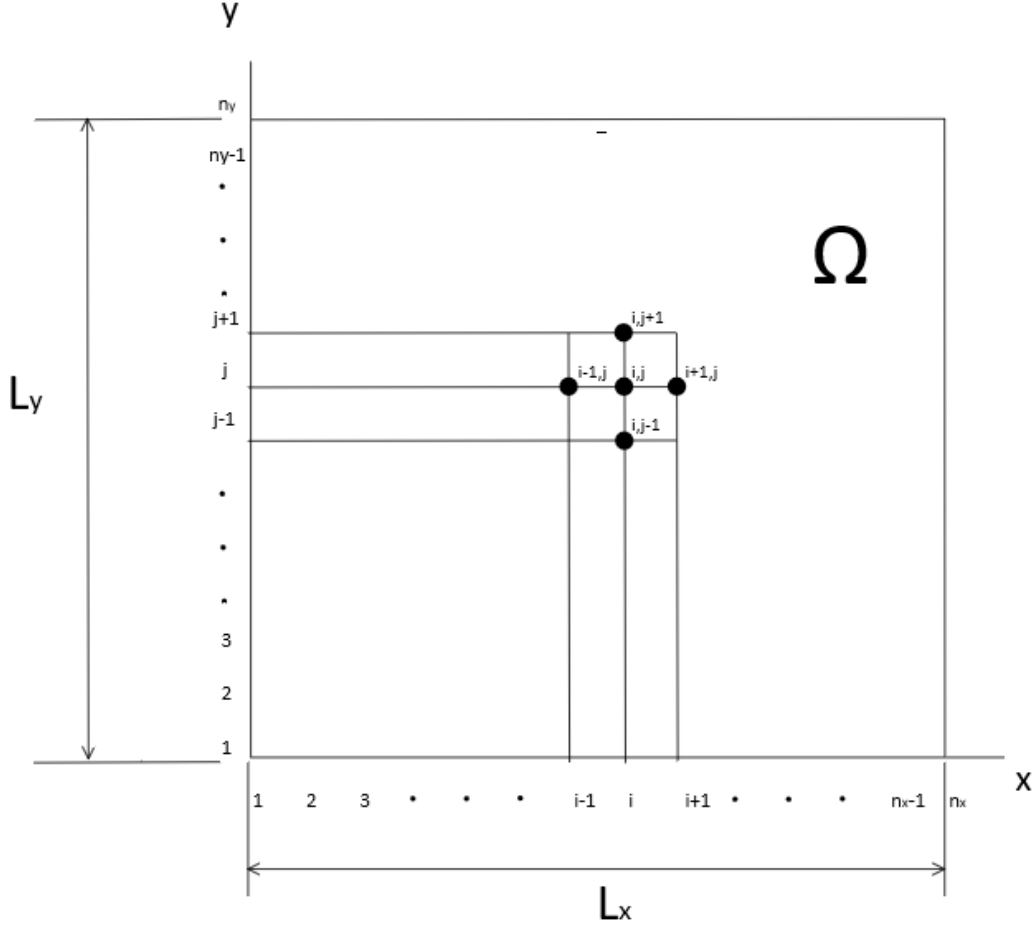


Figure 2: Spacial discretization of domain  $\Omega$ .

Moreover, for the temporal discretization, we consider the time index  $n$ , so our discrete time marks are going to be noted as  $t_n \forall n \in \{0, 1, 2, \dots, N\}$ . Therefore, we say that the initial time is at  $t = 0$ , meaning that  $t_0 = 0$ . In addition, we will note the final time as  $t_N = t_f$ .

When it comes to the distance between the points in the  $x$  and  $y$  directions, we will consider equally spaced points with distances given by  $\Delta x = x_{i+1} - x_i \forall i \in \{1, 2, \dots, n_x - 1\}$  and  $\Delta y = y_{j+1} - y_j \forall j \in \{1, 2, \dots, n_y - 1\}$ , while the temporal points will be equally spaced as well, with distances given by  $\Delta t = t_{n+1} - t_n \forall n \in \{0, 1, \dots, N - 1\}$ .

Since we seek to develop a generalized solution, we will use different discretizations in the  $x$  and  $y$  directions a priori (meaning that  $\Delta x$  is not necessarily equal to  $\Delta y$ ). Finally, using this discretization, we can say that the initial temperature in all nodes is  $T_{i,j}^0 = -3 \text{ } ^\circ\text{C}$ ,  $\forall (x_i, y_j) \in \Omega$ . Note that we will use the index on the top of the temperature to indicate the time in which we are analysing.

## 1.1 Finite Volumes Method

To further analyse this case, we are going to do an energy balance in a control volume around each node to obtain, explicitly, the temperature values for the next time step for all points in  $\Omega$ ,  $\forall n \in$

$\{0, 1, 2, \dots, N - 1\}$ . For this, we will need to analyse the equations for each type of node, since depending on the node, the control volume changes. Finally, before going for the equations, a quick side note: we are going to deduct all the equations with prescribed constant values for volumetric heat generation, in order to generalize the code as a whole, but for the application in the car, we need to make some changes that can be described later on.

### Interior Nodes

To analyse the interior nodes, We will consider a control volume around the generic node  $(i, j)$ ,  $\forall i \in \{2, \dots, n_x - 1\}$  and  $\forall j \in \{2, \dots, n_y - 1\}$ , with volume given by  $V_{cell} = \Delta x \Delta y \Delta z$ , where  $\Delta z$  is the depth of the window.

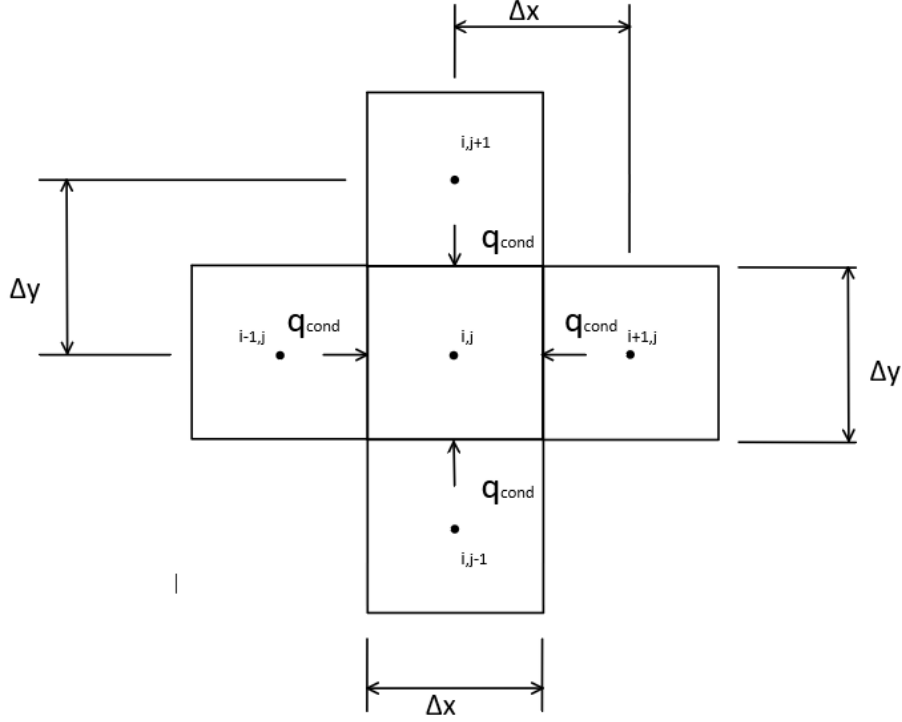


Figure 3: Control volume for the interior nodes of  $\Omega$ .

For the energy balance, we consider that  $q_{cond}$  is the heat rate flow by conduction and we also consider that all nodes  $(i, j)$  have a generic constant volumetric heat generation term, given by  $\dot{q}_{i,j}$ . Since the actual direction of heat flow (into or out of the node) is often unknown, it is convenient to formulate the energy balance by *assuming that all the heat flow is into the node*. Such a condition is, of course, impossible, but if the heat rate transfer equations are expressed in a manner consistent with this assumption, the correct form of the finite difference equations for all finite volumes is obtained. Therefore, we have generally

$$\dot{E}_{in} + \dot{E}_g = \dot{E}_{st} \quad (1)$$

Where  $\dot{E}_{in}$ ,  $\dot{E}_g$  and  $\dot{E}_{st}$  refers to the heat rate entering the control volume, the heat rate generation inside the control volume and the heat rate stored in the control volume, respectively. Thus, we find

$$\begin{aligned} \frac{k\Delta y\Delta z}{\Delta x} (T_{i-1,j}^n - T_{i,j}^n) + \frac{k\Delta y\Delta z}{\Delta x} (T_{i+1,j}^n - T_{i,j}^n) + \frac{k\Delta x\Delta z}{\Delta y} (T_{i,j-1}^n - T_{i,j}^n) + \frac{k\Delta x\Delta z}{\Delta y} (T_{i,j+1}^n - T_{i,j}^n) + \\ \dot{q}_{i,j}\Delta x\Delta y\Delta z = \frac{\rho c_p\Delta x\Delta y\Delta z}{\Delta t} (T_{i,j}^{n+1} - T_{i,j}^n) \end{aligned}$$

Note that the depth  $\Delta z$  can be neglected, since this term gets cancelled out in the equation. In fact, that occurs with every energy balance equation for all control volumes, so we can take the depth



In the case of the right boundary, we have convection with exterior air at temperature  $T_{infly} = -3$  °C and heat transfer coefficient  $h_o = 20$  W/(m<sup>2</sup>·K). To account for this in the energy balance, we need to add an additional term of heat by convection, using Newton's law of cooling for this. For the energy balance, we consider that  $q_{conv}$  is the heat rate flow by convection. Therefore, by using unitary depth, we find

$$\begin{aligned} \frac{k\Delta y}{\Delta x} (T_{n_x-1,j}^n - T_{n_x,j}^n) + \frac{k\Delta x}{2\Delta y} (T_{n_x,j-1}^n - T_{n_x,j}^n) + \frac{k\Delta x}{2\Delta y} (T_{n_x,j+1}^n - T_{n_x,j}^n) + \dot{q}_{i,j} \frac{\Delta x \Delta y}{2} + \\ h_o \Delta y (T_\infty - T_{n_x,j}^n) = \frac{\rho c_p \Delta x \Delta y}{2\Delta t} (T_{n_x,j}^{n+1} - T_{n_x,j}^n) \end{aligned}$$

By using the same definition as before for the Fourier number, by using the simplification of  $r = \frac{\Delta x}{\Delta y}$  and by defining the Biot number at outer surface  $B_{i,o} = \frac{h_o \Delta y}{k}$ , we arrive at the following expression:

$$\begin{aligned} T_{n_x,j}^{n+1} = 2Fo \left[ \frac{1}{r} T_{n_x-1,j}^n + \frac{r}{2} (T_{n_x,j-1}^n + T_{n_x,j+1}^n) + \dot{q}_{n_x,j} \frac{\Delta x \Delta y}{2k} + B_{i,o} T_\infty \right] + \\ \left[ 1 - 2Fo \left( r + \frac{1}{r} + B_{i,o} \right) \right] T_{n_x,j}^n \end{aligned} \quad (4)$$

Which stands valid  $\forall j \in \{2, 3, \dots, n_y - 1\}$  and  $\forall n \in \{0, 1, \dots, N - 1\}$ . Following the same stability criteria analysis as for the interior nodes, we have

$$1 - 2Fo \left( r + \frac{1}{r} + B_{i,o} \right) \geq 0 \quad (5)$$

### Left Boundary

The analysis is analogous to that seen for the right boundary, but now the wall is exposed to air flowing with a heat transfer coefficient of  $h_i = 6$  W/(m<sup>2</sup>·K). This way, we can define another Biot number, this time for the inner surface, which is given by  $B_{i,i} = \frac{h_i \Delta y}{k}$ . The equation found is pretty similar to that in the right wall, but with some changes in the indices. By analysing this region with equation 1, we find that

$$\begin{aligned} T_{1,j}^{n+1} = 2Fo \left[ \frac{1}{r} T_{2,j}^n + \frac{r}{2} (T_{1,j-1}^n + T_{1,j+1}^n) + \dot{q}_{1,j} \frac{\Delta x \Delta y}{2k} + B_{i,i} T_\infty \right] + \\ \left[ 1 - 2Fo \left( r + \frac{1}{r} + B_{i,i} \right) \right] T_{1,j}^n \end{aligned} \quad (6)$$

With a stability criteria pretty similar to the inequality 5, but now given by

$$1 - 2Fo \left( r + \frac{1}{r} + B_{i,i} \right) \geq 0 \quad (7)$$

### Upper boundary

This boundary is defined for all points  $(i, j)$  where  $i \in \{2, n_x - 1\}$  and  $j = n_y$ . In this boundary, we have adiabatic behavior, which means that heat flows only in the horizontal direction. Therefore, we have the following scheme to study for the energy balance:

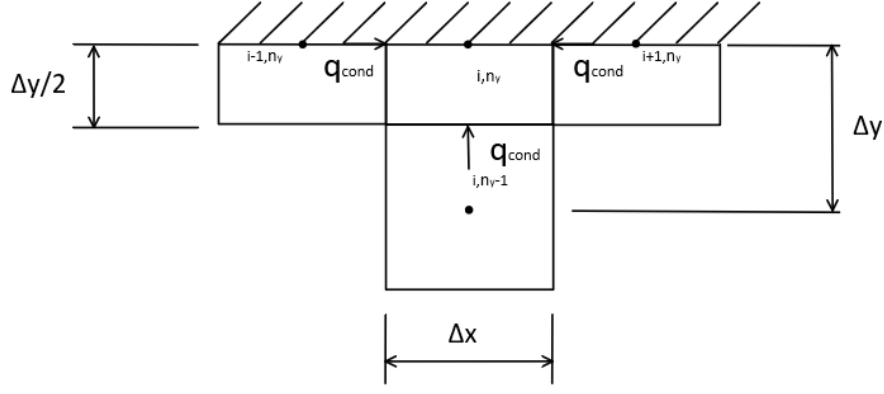


Figure 5: Control volume for the upper boundary nodes of  $\Omega$ .

By using the exact same energy balance approach, we arrive at the following expression:

$$T_{i,n_y}^{n+1} = 2Fo \left[ \frac{1}{2r} \left( T_{i-1,n_y}^n + T_{i+1,n_y}^n \right) + rT_{i,n_y-1}^n + \dot{q}_{i,n_y} \frac{\Delta x \Delta y}{2k} \right] + \left[ 1 - 2Fo \left( r + \frac{1}{r} \right) \right] T_{i,n_y}^n \quad (8)$$

With the same stability criteria as found for the interior nodes, given by 3.

### Lower Boundary

As for the left boundary, analysing the lower boundary is pretty analogous to analysing the upper boundary, with some minor changes in indices, but we end up with the same stability criteria as found for the interior nodes, given by 3. The equation found for the temperature at the next time step in this case is given by

$$T_{i,1}^{n+1} = 2Fo \left[ \frac{1}{2r} \left( T_{i-1,1}^n + T_{i+1,1}^n \right) + rT_{i,2}^n + \dot{q}_{i,1} \frac{\Delta x \Delta y}{2k} \right] + \left[ 1 - 2Fo \left( r + \frac{1}{r} \right) \right] T_{i,1}^n \quad (9)$$

### Top Right Corner

Now, we need to develop expressions for the temperature at the corners of  $\Omega$ . Beginning by the top right corner, we are at  $(i, j) = (n_x, n_y)$  and we have an adiabatic wall and a wall subjected to convection.

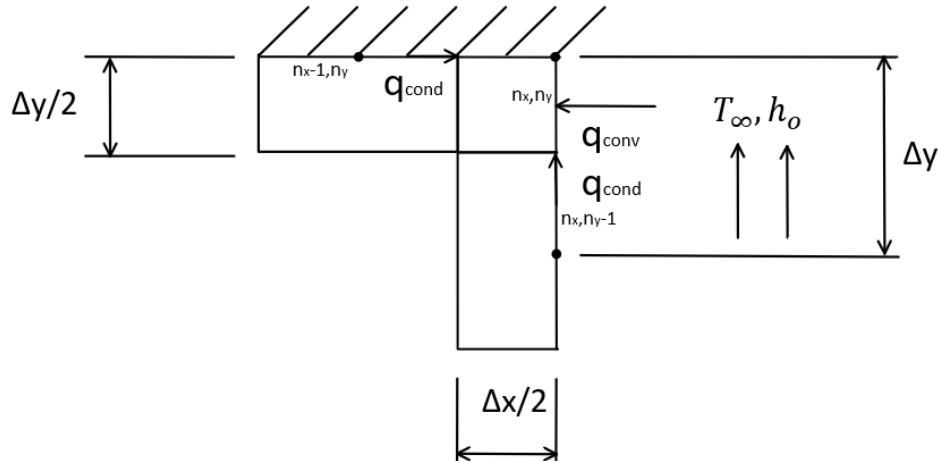


Figure 6: Control volume for the top right corner node of  $\Omega$ .

By using again the energy balance in the control volume, we arrive at the following expression:



$$T_{n_x, n_y}^{n+1} = 4Fo \left[ \frac{1}{2r} T_{n_x-1, n_y}^n + \frac{r}{2} T_{n_x, n_y-1}^n + \dot{q}_{n_x, n_y} \frac{\Delta x \Delta y}{4k} + \frac{B_{i,o}}{2} T_\infty \right] + \left[ 1 - 4Fo \left( \frac{r}{2} + \frac{1}{2r} + \frac{B_{i,o}}{2} \right) \right] T_{n_x, n_y}^n \quad (10)$$

And for this expression, the stability criteria is given by

$$1 - 4Fo \left( \frac{r}{2} + \frac{1}{2r} + \frac{B_{i,o}}{2} \right) \geq 0 \quad (11)$$

### Bottom Right Corner

Again, the analysis for this corner is analogous to that seen for the top right corner, with some minor changes in indices, but still with the same stability criteria as found for the top right corner. Thus, after doing an energy balance on the control volume at  $(i, j) = (n_x, 1)$ , we find that

$$T_{n_x, 1}^{n+1} = 4Fo \left[ \frac{1}{2r} T_{n_x-1, 1}^n + \frac{r}{2} T_{n_x, 2}^n + \dot{q}_{n_x, 1} \frac{\Delta x \Delta y}{4k} + \frac{B_{i,o}}{2} T_\infty \right] + \left[ 1 - 4Fo \left( \frac{r}{2} + \frac{1}{2r} + \frac{B_{i,o}}{2} \right) \right] T_{n_x, 1}^n \quad (12)$$

### Top Left Corner

One more time, we find ourselves analysing another similar case, but this time with convection heat transfer coefficient given by  $h_i$ , which means that the appropriated Biot number is given by  $B_{i,i}$ . After analysing the control volume at this corner, we find that

$$T_{1, n_y}^{n+1} = 4Fo \left[ \frac{1}{2r} T_{2, n_y}^n + \frac{r}{2} T_{1, n_y-1}^n + \dot{q}_{1, n_y} \frac{\Delta x \Delta y}{4k} + \frac{B_{i,i}}{2} T_\infty \right] + \left[ 1 - 4Fo \left( \frac{r}{2} + \frac{1}{2r} + \frac{B_{i,i}}{2} \right) \right] T_{1, n_y}^n \quad (13)$$

With stability criteria given this time by the following inequality:

$$1 - 4Fo \left( \frac{r}{2} + \frac{1}{2r} + \frac{B_{i,i}}{2} \right) \geq 0 \quad (14)$$

### Bottom left corner

Last, but not least, we have the bottom left corner. Again, by using the energy approach, the analysis is pretty much the same as for the top left corner, and indeed with the same stability criteria as in 14, but with a slight change in indices. We have that

$$T_{1, 1}^{n+1} = 4Fo \left[ \frac{1}{2r} T_{2, 1}^n + \frac{r}{2} T_{1, 2}^n + \dot{q}_{1, 1} \frac{\Delta x \Delta y}{4k} + \frac{B_{i,i}}{2} T_\infty \right] + \left[ 1 - 4Fo \left( \frac{r}{2} + \frac{1}{2r} + \frac{B_{i,i}}{2} \right) \right] T_{1, 1}^n \quad (15)$$

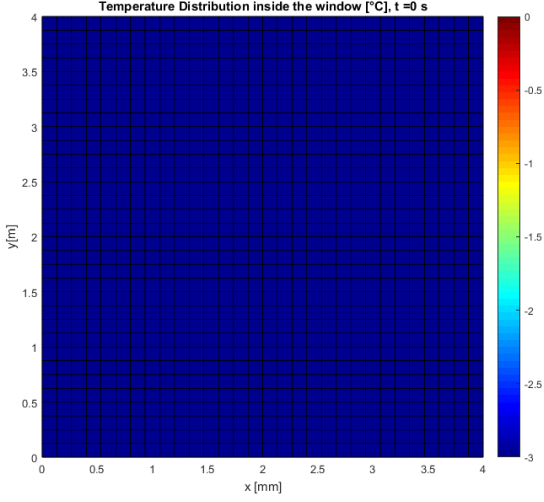
## 2 Numerical Simulation: Results

Using the numerical data given and the code written in MATLAB designed to analyse this project, named "project\_main\_Raphael\_Alves\_Hailer.m", gives us the possibility to actually check if the heating wires are in fact defrosting the car's rear window or not. For the simulation, it has been chosen a final time  $t_f = 120$  s,  $n_x = 31$ ,  $n_y = 33$  and  $\Delta t = 0.01$  s. For this configuration, we can already have a high precision in the results, due to the fine mesh generated. In the code, it is also possible to check on the calculations for the heat flux at each point on the grid, which is normalized and plotted as a vector field on top of the temperature distribution, in order to see the direction of heat flux flowing through the window. Furthermore, there is an option inside the code to see a little animation of the temporal evolution as the time steps grows bigger.

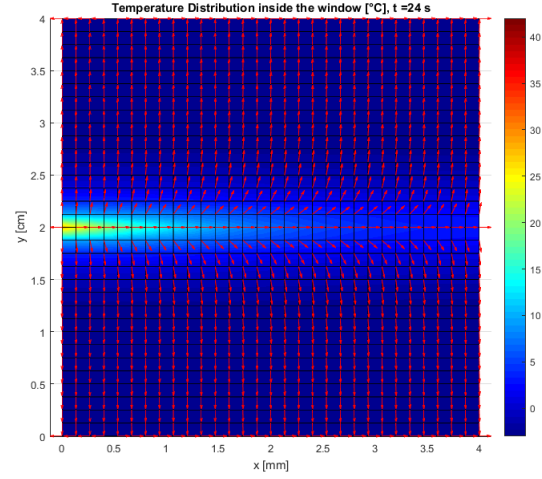
It is also noticeable that the finer the mesh, the better are the results, because numerical errors will diminish as  $\Delta x$ ,  $\Delta y$  and  $\Delta t$  gets smaller, but we must lookout for the stability criteria obtained in each type of control volumes throughout the nodes in  $\Omega$ .

Another thing to look out when it comes to comparing the code to the theoretical deduction made in this report, it is crucial to mention that the deductions of the report were made considering volumetric heat generation inside the nodes. In the case of the car, we have heat generation by unit of depth. Therefore we should consider that for each energy balance equation, we should start with heat generation  $\dot{E}_g = q' \Delta z$ , and since we can consider unitary depth for the calculations, then we only need to consider the value of  $q'$ , which stands for heat generation for unit depth.

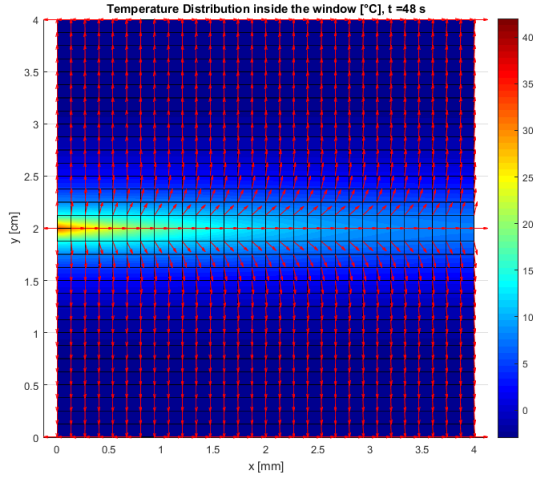
Moreover, in the case of the car's rear window, actually we only need to include the heat generation term for one node, but the code can be used for more general purposes too, since we can change the distribution of heat generation throughout the glass and experiment with new configurations.



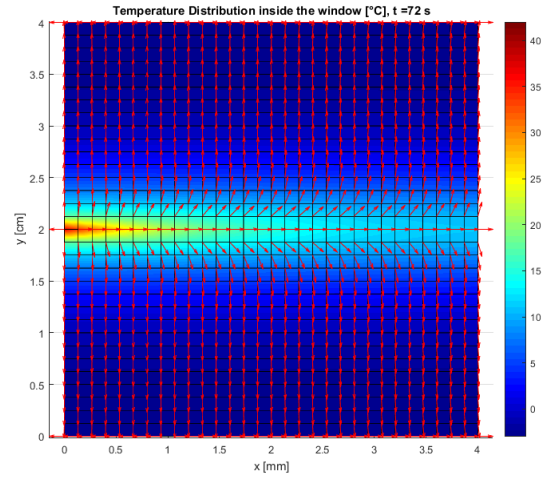
(a) Initial temperature distribution



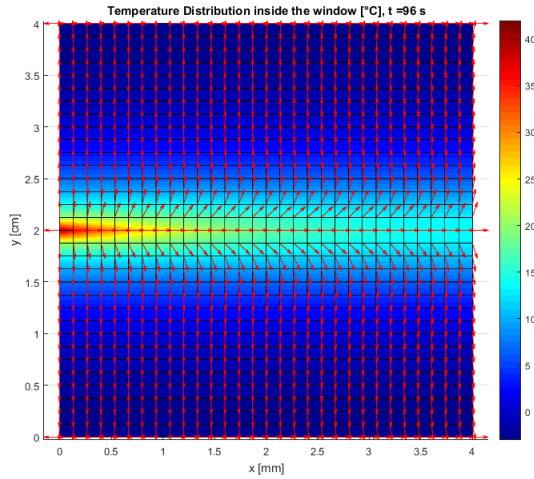
(b) Temperature distribution for  $t = 24$  s.



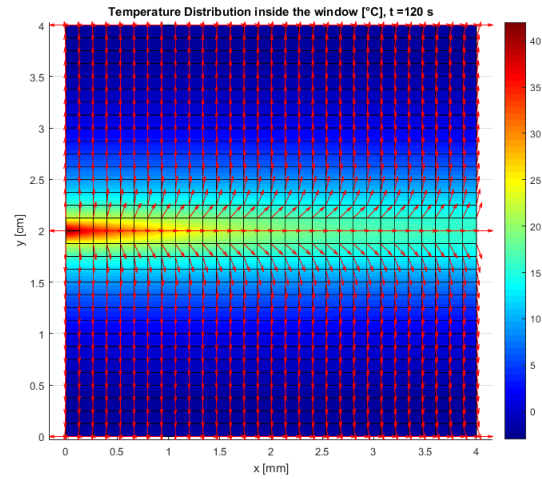
(c) Temperature distribution for  $t = 48$  s.



(d) Temperature distribution for  $t = 72$  s.



(e) Temperature distribution for  $t = 96$  s.



(f) Temperature distribution for  $t = 120$  s.

Figure 7: Temporal evolution of the temperature distribution on the car's rear window

Furthermore, we can see that with these physical parameters and considering the internal temperature of the car remaining at  $T_\infty$ , we conclude that the heating wires are inefficient. Nevertheless, the approximation made for the constant internal temperature of the car is not appropriated after a long period of time, because the heating wires are going to heat up the air close to the window, providing the defrosting effect desired. For comparison effects in further analysis, we found in this case that  $T_{min} = -2.24$  °C and  $T_{max} = 41.43$  °C

On top of that, the observed behaviour can be misleading by the naked eye, because of the scale of the axis. Since we have  $L_y = 10L_x$ , we should be using more points in the y direction, to better visualize the effect of conduction in this sense. Additionally, it is expected to observe a circular heat spreading in the wall, but we must remember that the thickness of the wall is very small, so we need to adjust the scale of the axis. By doing it so, for the same parameters but only for the final time of 120 s, we find that the heat spreads in the way expected.

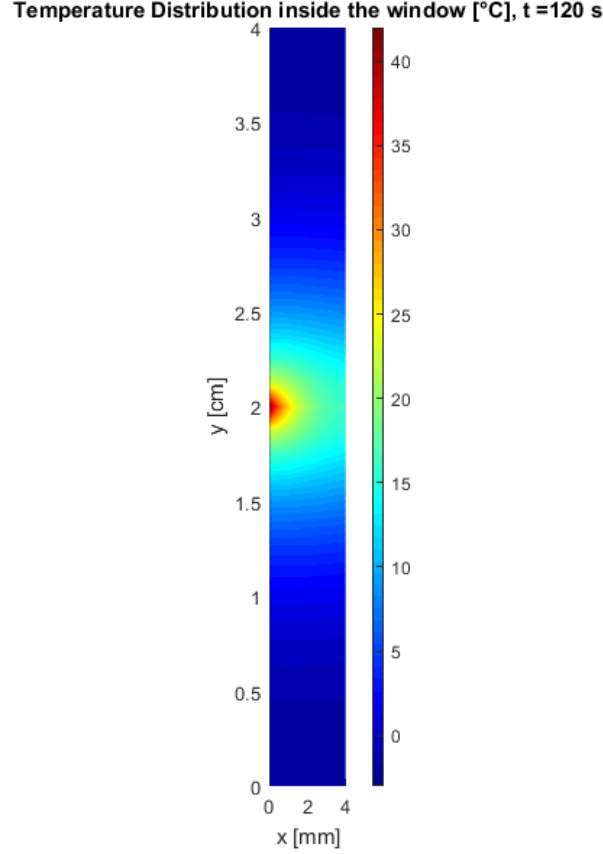


Figure 8: Temperature distribution at  $t = 120$  s after correcting the aspect ratio of the x and y axis

Moreover, it is remarkable to point out that by not following the stability criteria, the results explode to infinity, so when this happens, it is often useful to look for ways to diminish the Fourier number, by increasing the values of  $\Delta x$  or  $\Delta y$  (by manipulating the values of  $n_x$  and  $n_y$ ) as well as trying to diminish the value of  $\Delta t$ . One such example of unstable response is provided, for the same mesh configurations but with final time of only 2 seconds. We can see that only 2 seconds of simulation is more than enough to conclude that the method is unstable. In fact, the explicit method for time evolution is, unfortunately, not unconditionally stable.

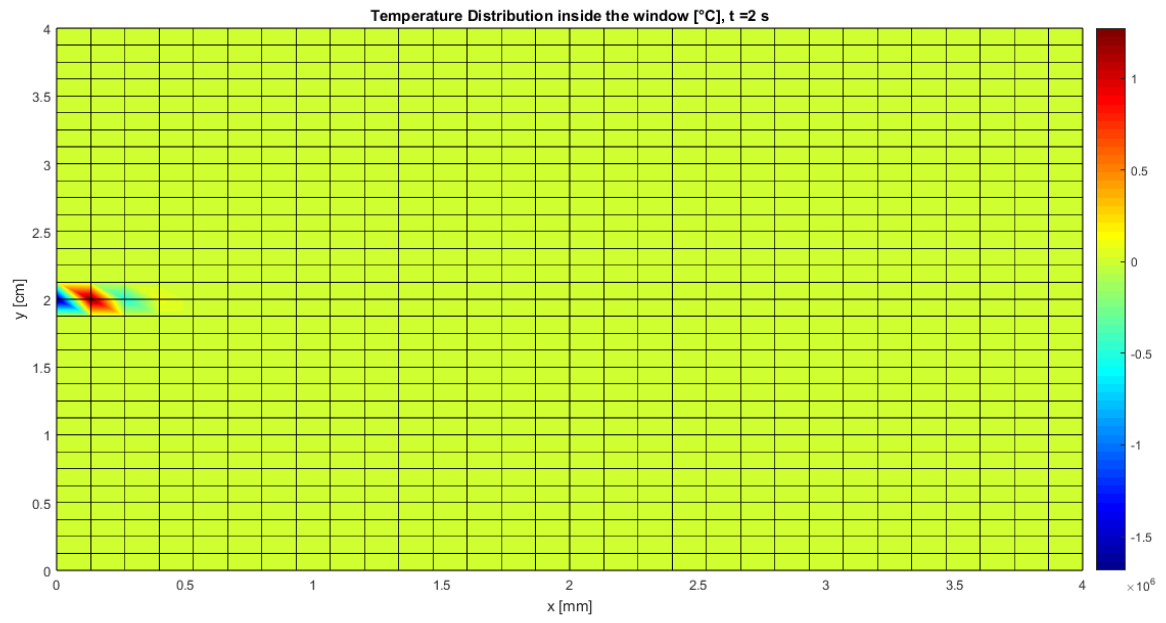
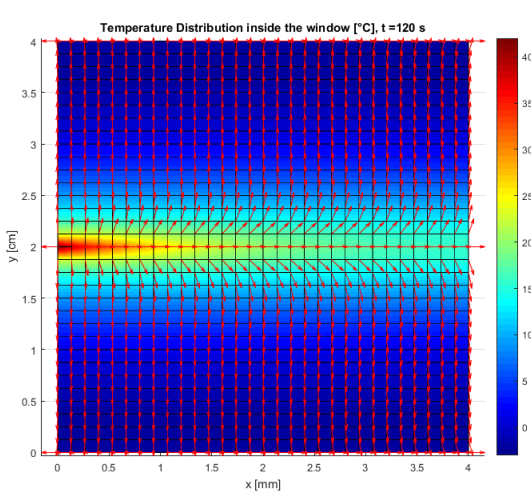


Figure 9: Unstable response for inappropriate discretization values.

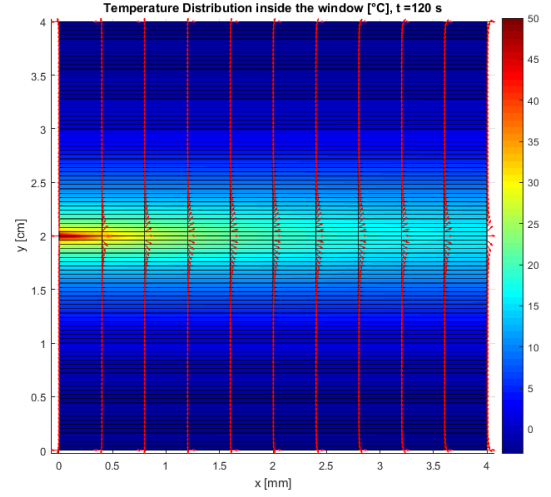
### 3 Experimenting With New Parameters

In order to better understand the behaviour of the car's rear window as we turn on the heating wires, it is appropriated to use more nodes in the vertical direction, while for the horizontal direction we are going to use a few nodes only. To compare results, we are analysing only the response at a final time, not the evolution as a whole.

For this evaluation, consider  $n_y = 101$ ,  $n_x = 11$  and  $\Delta t = 0.01$ . For  $t_f = 120$  s, the results obtained show that in reality a higher maximum temperature is obtained ( $T_{max} = 48.98$  °C), but we still have negative temperatures along the window ( $T_{min} = -2.25$  °C), which means that the window is not defrosting entirely. But in general, the heat spreading is occurring in the same manner as before, but now we have higher precision. Therefore, unrefined meshes still produces good qualitative results, but poor quantitative results.



(a)  $n_x = 31$  and  $n_y = 33$ .



(b)  $n_x = 11$  and  $n_y = 101$ .

Figure 10: Comparison between rougher and finer mesh.

In order to defrost the car's rear window, a good approach is to increase the number of heating wires, which means to diminish the value of  $L_y$ , since the spacing between them are going to get smaller. Therefore, by choosing  $L_y = 2$  cm, which is equal to saying that we are doubling the number of heating wires, we obtain maximum and minimum temperatures of 51.99 °C and 5.82 °C, respectively. Therefore, by increasing the heating wires number, we can achieve the desired effect of defrosting.

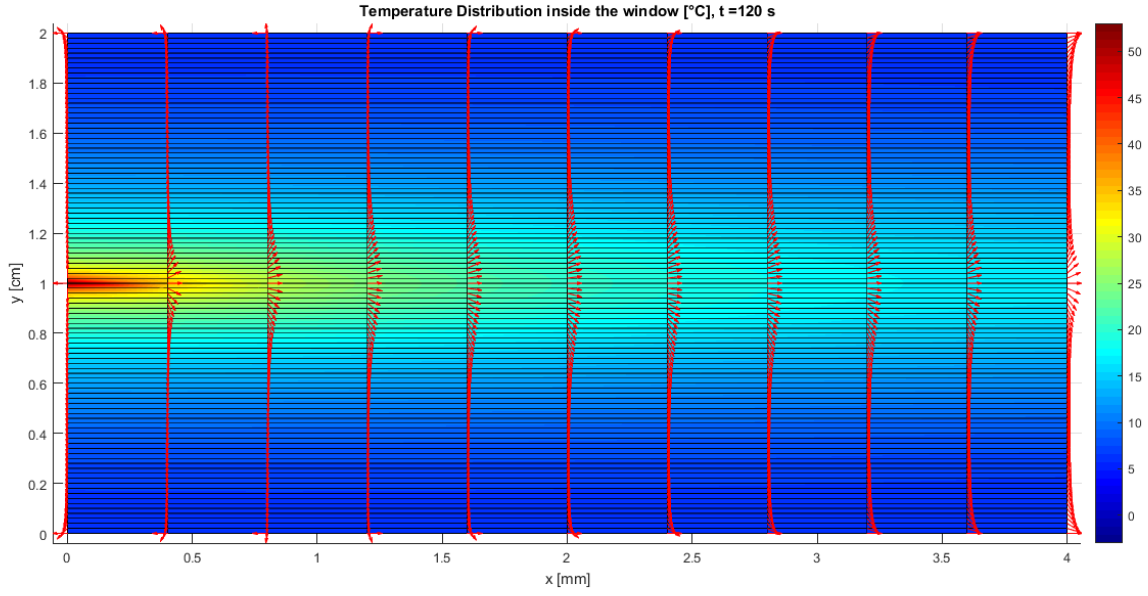


Figure 11: Temperature distribution after 120 seconds with  $L_y = 2$  cm.

The option of diminishing  $L_y$  by increasing the number of heating wires is actually the only viable option, because we cannot control the physical parameters of the car's rear window, such as diffusivity and thermal conductivity values. But, for academical reasons we can check what happens if we increase the value of  $k$ , and consequently  $\alpha$ . By tripling the value of  $k$ , and by consequence tripling the value of  $\alpha$ , we find that heat spreads way more easily inside the window, giving a more uniform spread to the thermal energy provided by the heating wires. In this configuration, we find  $T_{max} = 20.76$  °C and  $T_{min} = 0.7$  °C, while keeping  $L_y = 4$  cm.

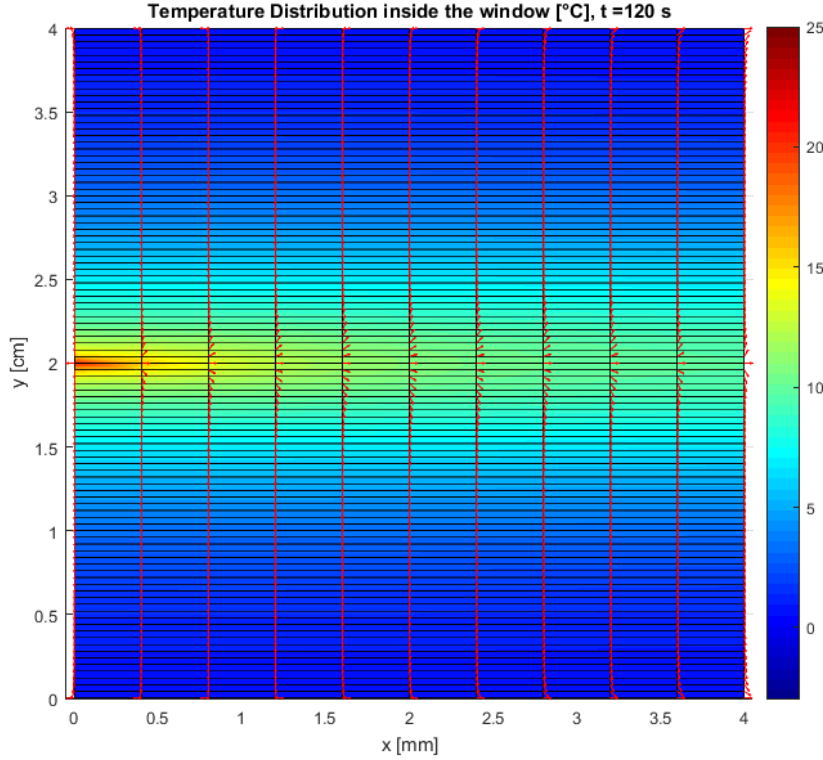


Figure 12: Temperature distribution after 120 seconds with  $k = 2.52$  W/(m·K).

Indeed, many physical aspects can bring changes to the heat conduction response of the window,

and the code provided along with this report can be modified to new configurations and studies, even with volumetric heat generation inside  $\Omega$ . We can see that having more heating wires is a possibility to achieve defrosting of the car's windows, as well as using glass with at least 3 times higher thermal conductivity. Nevertheless, using the initial configuration is not enough to defrost the entire window.